Hot-gas flow and particle transport and deposition in a candle filter vessel

ALI REZA MAZAHERI [t], GOODARZ AHMADI [t],* and ISAAC K. GAMWO [z]

[t] *Department of Mechanical and Aeronautical Engineering Clarkson University, Potsdarn, NY 13699, USA*

[z] *US Department of Energy, National Energy Technology Laboratory, PO Box 10940, Pittsburgh, PA 15236-0940, USA*

Received 1 March 2002; accepted 24 July 2002

Abstract--Hot-gas flow and particle transport and deposition in an industrial filtration system are studied. The special example of the Siemens-Westinghouse filter vessel at the Power System Development Facility at Wilsonville, Alabama is treated in detail. This tangential flow filter vessel contains clusters of 91 candle filters, which are arranged in two tiers. The upper tier containing 36 candle filters is modeled by six equivalent filters. Seven equivalent filters are used in the computational model to represent the 55 candle filters in the lower tiers. The Reynolds stress turbulent model of FLUENT'" code is used, and the gas mean velocity and root mean square fluctuation velocities in the filter vessel are evaluated. The particle equation of motion used includes drag and gravitational forces. The mean particle deposition patterns are evaluated and the effect of particle size is studied. The computational results indicate that large particles of the order of 10 hm or larger are removed from the gas due to the centrifugal forces exerted by rotating flow between the shroud and the refractory.

Keywords: Hot-gas; particle transport; deposition; ash deposition.

1. INTRODUCTION

Developing advanced clean coal technology for electric power generation with high efficiency and low pollutants has seen considerable interest in recent years. As a result, advanced pressurized fluidized bed combustion (PFBC) and integrated gasification combined cycles (IGCC) are being developed and tested as part of the Clean Coal Technology Program of the US Department of Energy. These highly efficient advanced coal energy systems require effective removal of ash and the unreacted and reacted sulfur sorbent from the hot gases.

*To whom correspondence should be addressed. E-mail: ahmadi@clarkson.edu

The procedure for cleaning hot gases has been focused on the use of ceramic candle filters. In practice, an industrial filter vessel contains several hundred candle filters. Dust cake builds up on the filters during the operation of the system. Groups of candle filters are periodically cleaned by a back-pulse procedure. In the past decade, a number of pilot- and demonstration-scale hot-gas filtration systems have been developed and tested. Rockey *et al. [1]* described the operation data of the National Energy Technology Laboratory (NETL) Integrated Gasification and Cleanup Facility (IGCF). The filter vessel in this unit supported up to four candle filters. Smith *et al. [2-5]* analyzed the IGCF operational data and presented simple models for time variation of filter pressure drop and cake buildup. Mudd and Hoffman [6, 7] described the operation of the Westinghouse Advanced Particle Filter (APF) that was installed at the Tidd PFBC Demonstration Plant at Brilliant, Ohio. Lippert *et al.* [8-10] also reported the test results of the Tidd filtration system. The composition and chemistry of particles in the Tidd filter vessel were also studied by Southern Research Institute [11], Pontius [12], Hurley [13], Chiang (pers. commun.) and Smith *et al. [3].* The Siemens-Westinghouse Particulate Control Device (PCD) at the Power System Development Facility (PSDF) at Wilsonville, Alabama was described by Davidson *et al. [14].*

Thambimuthu [15] and Clift and Seville [16] provided extensive reviews of gas cleaning at high temperatures. Recent developments on hot-gas cleaning with the use of ceramic candle filters were described by Schmidt *et al.* [17] and Dittler *et al. [18].* Smith and Ahmadi [19] discuss the progress and issues concerning hot-gas filtration in connection with the PFBC and IGCC systems. While candle filters generally have a very high cleaning efficiency of the order of 99%, there are still a number of unresolved issues with buildup of dust cake on the filters, occasional filter-ash bridging, and filter failure and breakage.

In order to improve the reliability of hot-gas filtration systems in commercial applications, a fundamental understanding of the ash transport and deposition processes in the filter vessels is needed. Considerable progress has been made on the mechanisms that control dispersion and deposition of particles in gas flows. Accordingly, the particles are converted by the mean motion, and are dispersed by the Brownian motion and turbulence fluctuation velocities. Semi-empirical expressions for the particle deposition rate were developed by Friedlander and Johnstone [20], Cleaver and Yates [21], Wood [22, 23], Hinds [24], Hidy [25], Papavergos and Hedley [26] and Fan and Ahmadi [27]. A computational model for simulating deposition of aerosols in complex passages was developed by Li and Ahmadi [28-30] and He and Ahmadi [31]. Recently, Ahmadi and Smith [32, 33] described the results of their computer simulations on the deposition of particles in the NETL-IGCF pilotscale filter vessel and the filter vessel at the Tidd 70 MWE PFBC Demonstration Power Plant. More recently, Zhang and Ahmadi [34] reported a computer simulation study of gas flow and particle deposition in the hot-gas filter at Wilsonville, Alabama. The corresponding thermal effects were discussed by Gamwo *et al. [35].*

In this work, particle transport and deposition in a tangential flow hot-gas filtration device is studied. Particular attention is given to the Siemens-Westinghouse PCD at the demonstration-scale PSDF in Wilsonville, Alabama. To be able to assess the effect of strong tangential flow in the vessel on the deposition pattern of different size particles, a refined grid was generated and used in the analysis. The Reynolds stress turbulence model of the FLUENT ™ code is used for evaluating the gas mean velocity and the root mean-square fluctuation velocity in the filter vessel. The deposition patterns of ash particles of different sizes are evaluated. The particle equation of motion including the drag and the gravitational forces are used in the simulation. The results show that the centrifugal forces generated by the rotational motion significantly affect the transport and deposition of large particles. In particular, a large fraction of 10 gm particles (or larger) deposit in the region between the shroud and the vessel refractory.

2. HOT-GAS FILTER VESSEL

The special case studied is that of the Siemens-Westinghouse tangential flow hot-gas filter vessel that is currently being tested at the Southern Research Company Facility (PSDF) at Wilsonville near Birmingham, Alabama. This PCD is 1.6 m (63 in.) in diameter and 8.27 m (325.7 in.) long. The vessel accommodates 91 candle filters arranged in two clusters. The upper and lower tiers have, respectively, 36 and 55 candle filters. The ceramic candle filters are about 6 cm (2.36 in.) in outer diameter and 1.5 m (4.92 ft) long. A special feature of the PCD at Wilsonville is that the hot gas enters the vessel tangentially into the vessel. There is a large cylindrical shroud in the vessel and the inlet hot gas flows in the gap between the vessel refractory and the shroud. The purpose of the shroud is to distribute the incoming gas in the body of the filter vessel and also to avoid impingement of the high-speed inlet gas directly on the ceramic candle filters. Figure 1 shows a schematic of the Siemens-Westinghouse PCD.

The average gas mass flow rate into the filter vessel is 2.95 kg/s (23 500 lb/h), with the PCD operating at a pressure of 1344 kPa (195 p.s.i.a.) and a temperature of 1033 K (760°C). Under these operating conditions, the corresponding inlet flow velocity is 9.8 m/s, the air density is 4.53 kg/m^3 and the air viscosity is 3.7 x 10^{-5} kg/ms. The solid volume fraction at the inlet is typically about 0.005-0.025. Therefore, the flow in bulk of the filter vessel is rather dilute.

3. EQUIVALENT FILTER

To keep the computational effort manageable, the group of 36 candle filters in the upper tier is modeled by six equivalent filters and the 55 lower filters are replaced by seven equivalent cylindrical filters. The lengths of the equivalent filters are all identical to that of the actual candle filters. All equivalent cylindrical filters, except for the one at the center of the lower cluster, have an outer diameter of 28.9 cm

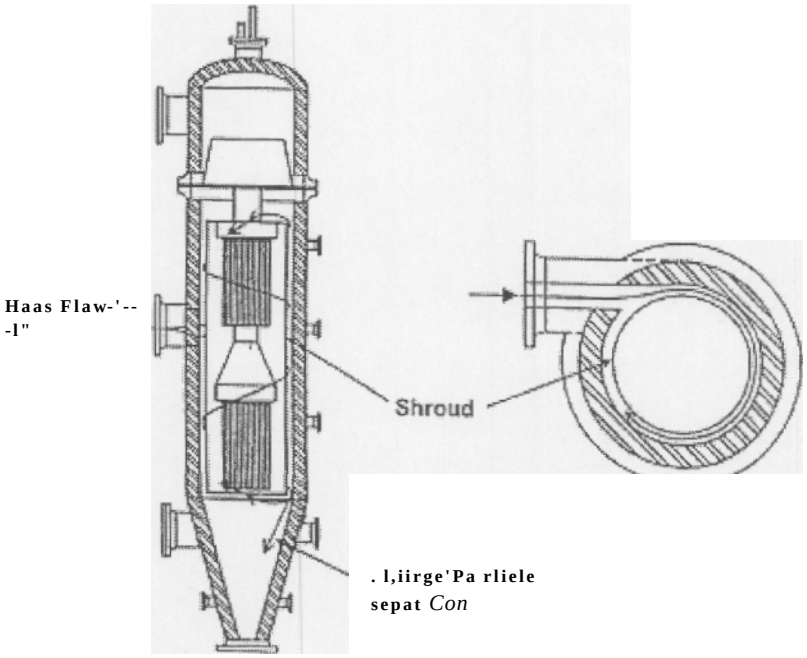

Figure 1. Schematic of the Siemens-Westinghouse PCD at

(11 in.) and inner diameter of 23.9 cm (9.4 in.). The one at center of the lower tier has an outer diameter of 40.6 cm (16 in.) and an inner diameter of 34.5 cm (13.6 in.). Figure 2 shows the schematics of the filter vessel with the equivalent filters used in the computation.

The equivalent filter diameters are selected in such a way to maintain the size and symmetry of the arrangement of groups of six ceramic filters. The permeability and the thickness of the effective cylindrical filters are adjusted so that they have the same pressure drop as the actual candle filters. The use of the seven equivalent filters in the lower tiers and six in the upper tier maintain the proper flow distribution between these filter clusters. Assuming that the candle filters have a permeability of 10^{-12} m'- , the effective permeability of the upper and lower 28.9 cm equivalent filters is 2.033 x 10^{-12} m^2 and of the 40.6 cm equivalent cylindrical filter at the center of the lower tier is 3.05 x 10-12 m2.

It should be noted here that the use of six equivalent filters in the upper tier and seven equivalent filters in the lower tier is an important improvement over the earlier work of Zhang and Ahmadi [34] (Fig. 3). The present model provides for a proper distribution of the available filtration surface area between the upper and lower tiers. Thus, it is expected that the computed flow patterns provide for a more realistic representation of the condition in the Siemens-Westinghouse PCD.

It should be emphasized that in the present study a uniform permeability for the candle filers is assumed. However, it is known that the permeability could also vary spatially and various regions of a candle filter or groups of filters could have

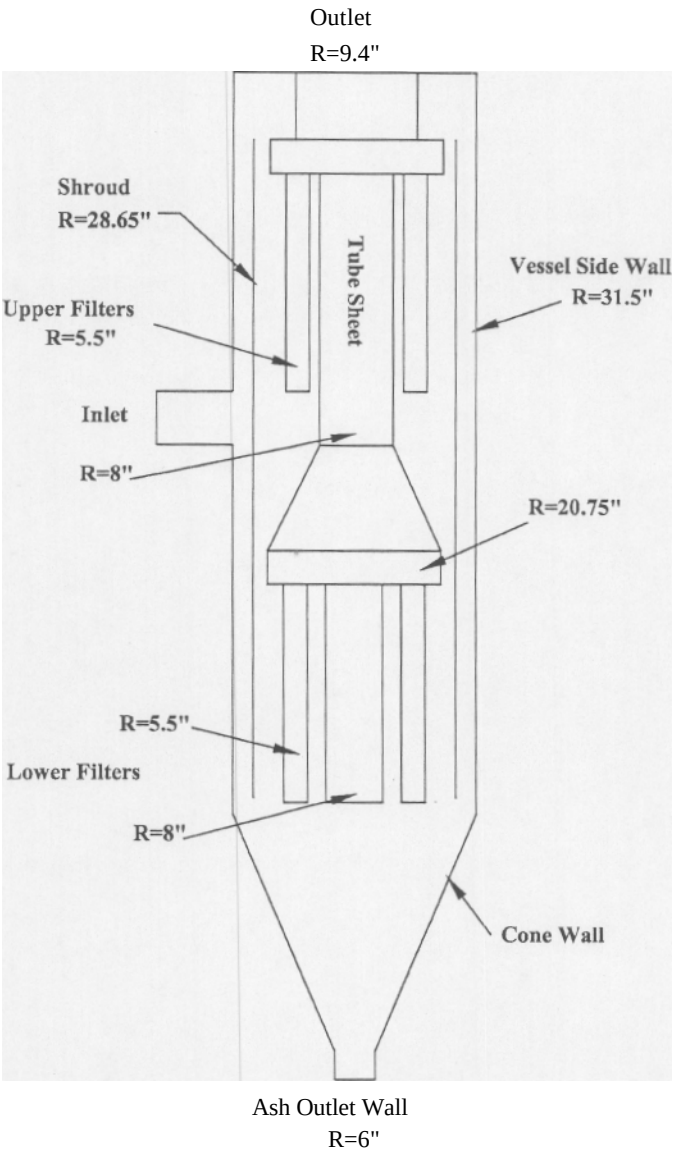

Figure 2. Schematic of the modeled filter vessel.

different permeabilities depending on their location. This could be the case when different kinds of candle filters are being tested or due to incomplete cleaning [2-5]. These additional refinements, however, are not considered in the present study.

Figure 2 identifies various surfaces of the PCD vessel for future reference in the text. The outer walls of the system are divided into four parts, the `upper wall', the `vessel side wall', the `cone wall' and the `lower wall'. The `vessel side wall' denotes the straight part of the outer walls, which is about the length of the shroud. The `upper wall' denotes the part of the vessel wall, which is above the

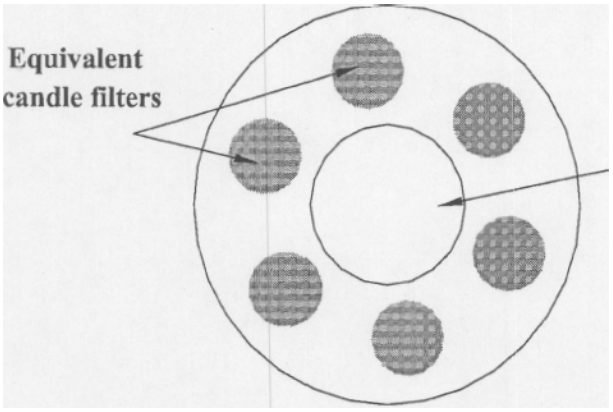

a. Upper tier

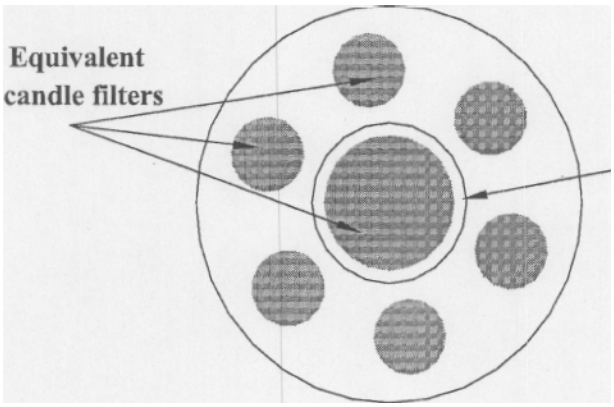

b. Lower tier

Figure 3. Schematics of the effective candle filters used in the simulation.

wall'. The `cone wall' denotes the conical section of the wall below the `vessel side wall'. The `ash outlet wall' is the wall of the ash collection passage at the bottom of the vessel. The `shroud wall' denotes the shroud surface. The `tubesheets', are the parts to which the candle filters are attached. The `connecting post' connects the upper and the lower tubesheets.

4. SIMULATION PROCEDURE

4.1. Gas flow simulation

The simulation makes use of the Reynolds stress transport model of FLUENT^{Tm} version 5 *(FLUENT User's Guide 1998*, vol. 2) for evaluating the turbulent gas

condition in the filter vessel. In an earlier work, Ahmadi and Smith [32, 36] showed that the temperature and density of gas do not vary appreciably in the NETL hotgas filtration vessel. Similar to Zhang and Ahmadi [34], for the present PCD, we assume that variations of gas density and temperature to be comparatively small, and the incompressible fluid option with a constant density and temperature is used in the simulation.

It should be emphasized that the entire filter vessel from the inlet to the gas exhaust at the top of the vessel is simulated. In particular, the. ceramic filters are treated as porous media with a given permeability and the penetration of the gas through the filter wall is computed as part of the solution (i.e. there was no imposed boundary condition at the filter surface).

4.2. Lagrangian particle trajectory

We used the particle equation of motion of the code including drag and gravitational forces in the analysis. It is known that the drag force is generally dominant and the effect of fift force is small [34]. As noted before, the mean gas velocity in the PCD is first evaluated with the use of the Reynolds stress transport model. The resulting mean flow field was then used for the mean particle trajectory analysis.

5. SIMULATION RESULTS

The gas flow and ash particle transport and deposition in the Siemens-Westinghouse filter vessel at the PSDF at Wilsonville, Alabama are described in this section. The simulated turbulent gas flow field is first discussed. This is followed by an analysis of different size ash particles that enter the vessel at the inlet.

5.1. Computational grid

Due the rather complex geometry of the PCD, an unstructured grid of 1371162 cells generated by GAMBIT code is used in the simulations. To allow a more accurate analysis of ash transport and deposition in the spacing between the shroud and vessel wall, the grid is further refined in these regions. Figure 4 shows the surface grid of the equivalent filters and at the mid-section of the vessel. In the computational model, the origin of the coordinate system is set in the center of the top of the vessel. The z-axis is in the vertical direction pointing downward (along the gravitational direction) and the x-axis is along the inlet flow direction.

5.2. Gas flow

Figure 5 shows the velocity vector plot in a plane at the mid-section of the vessel. Figure 5 shows that about half of the inlet gas moves upward in the shroud and the other half moves downward. Thus, the hot-gas enters the body of the vessel both from the top and the bottom of the shroud. The flow velocity is downward and

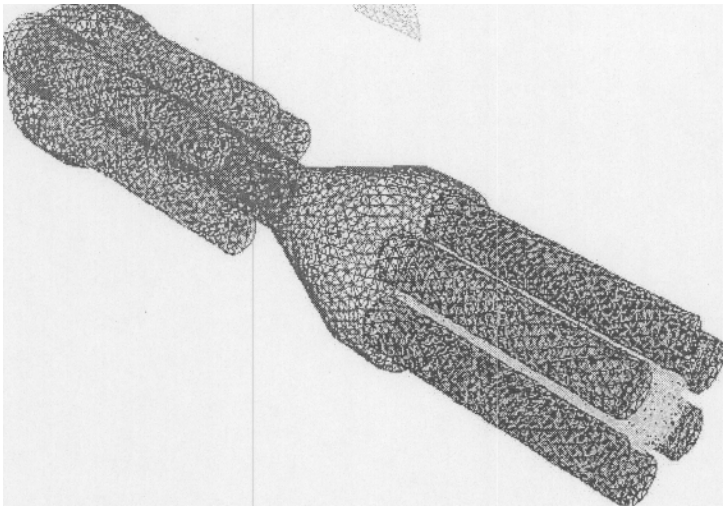

Figure 4. Grid schematic of the modeled filter vessel.

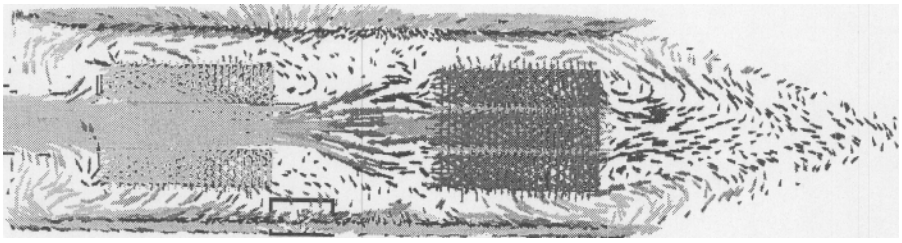

Figure 5. Velocity vector plot at the vessel mid-section.

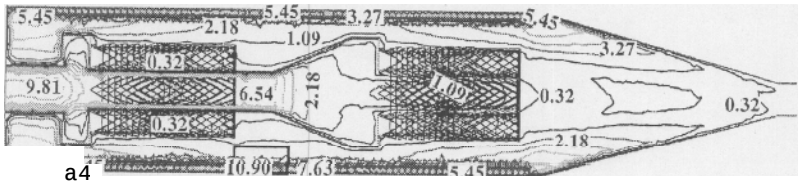

a4

Figure 6. Mean velocity magnitude contours at the vessel mid-section.

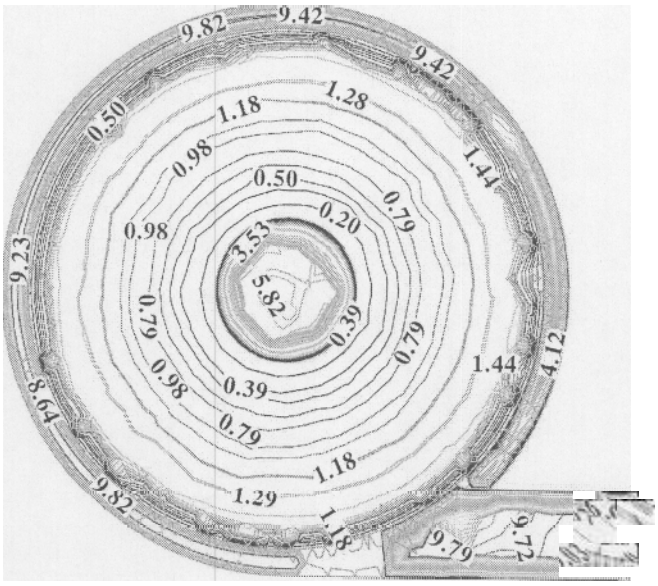

Figure 7. Mean velocity magnitude contours in a plane across the vessel and through the inlet.

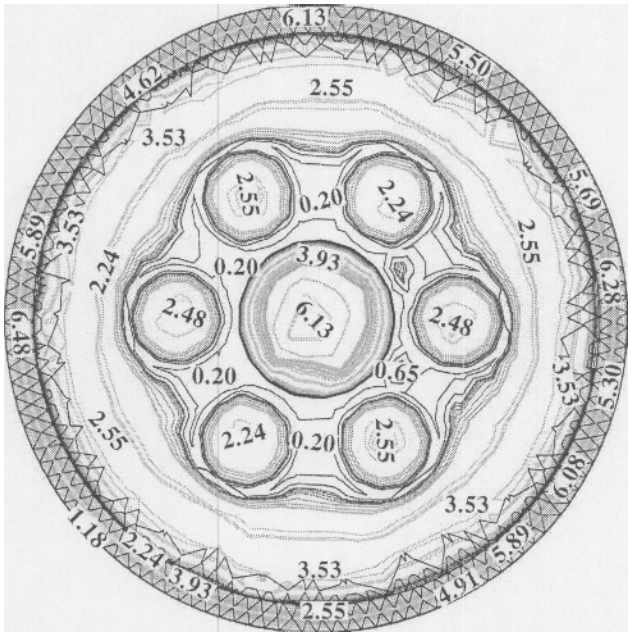

Figure 8. Mean velocity magnitude contours in a plane across the upper filters.

somewhat larger in the region between the upper filter and the shroud. Near the top of the vessel, the upward gas flow in the shroud turns sharply downward to enter the mean body of the vessel. Also, the downward gas flow near the outlet of the shroud at the bottom turns upward to enter the main body of the vessel. Recirculating flow regions in the lower conical part are clearly seen from Fig. 5.

Figure 6 shows the mean velocity magnitude contours in a plane at the mid-section of the PCD vessel. It is observed that the gas velocity inside the vessel is quite low, about 0.3-3 m/s, while is generally high, about 5-10 m/s, in the region between the vessel wall and the shroud.

Figure 7 shows the mean velocity magnitude in the plane that passes through the inlet at the x-y plane. As expected, there is a strong rotating flow condition through the shroud. Figure 7 also shows when the gas enters the body of the filter vessel from the shroud passage, it carries sufficient angular moment to sustain a noticeable rotational motion.

The mean velocity magnitude at the sections across the upper and lower filters is, respectively, shown in Figs 8 and 9. Figures 8 and 9 show that the velocity of the gas decreases across the candle filters. The gas then penetrates into the candle filters and the gas velocity somehow increases inside of the filters and especially inside the tube sheet.

Figure 10 shows the contour plots for variations of the static pressure in a plane at the mid-section of the PCD vessel. Figure 10 shows that the pressure remains almost constant inside the shroud and in the main body of the vessel. It is also shown that the main pressure drop occurs across the filter wall, and the pressure decreases inside the filter cavity. The air pressure inside the filter cavity and connecting pipes is roughly constant with a slight decrease toward the vessel outlet. The sharp pressure drop across the filter wall it is also clearly seen. It should be noted that in the body of the filter vessel the pressure is high and roughly uniform, and reduces significantly as the gas passes through ceramic filter wall and enters the candle filter cavity.

Variation of the turbulence kinetic energy in a plane at the mid-section of the filter vessel is shown in Fig. 11. The turbulence kinetic energy is generally quite low in the vessel except for certain regions inside the connecting tube.

5.3. Particle trajectory analysis

Particle transport and deposition in the Wilsonville filtration system are studied using the FLUENT code. Particles with diameters of 1, 10 and 30 Am with a constant density of 2700 kg/m^3 are used in these computer simulations, and 348 particles of different sizes are uniformly released at the inlet with the same velocity as the gas flow. The uniform particle source is a reasonable assumption for the particle concentration condition in the inlet during the operation of the filter vessel. In these simulations, the stick boundary condition is assumed for all surfaces. For each particle size, ensembles of trajectories are evaluated, and the particle deposition patterns on the different tier filters and various surfaces are analyzed.

5.4. Deposition rate

Table 1 shows the percentages of deposited 1 Am particles on various surfaces. Table 1 shows that about 8% of the particles are deposited on the upper filters, while about 40% of the particles are deposited on the lower filters. More importantly, about 38% of particles are deposited on the vessel wall and on the outer surface of shroud. Furthermore, it is observed that the total deposition rate on the lower filters is higher than that on the upper filters. While the particle size is small, the results show that the centrifugal force affects significantly the particle deposition rates on the areas between the vessel wall and the shroud.

Table 2 shows the simulation results for 10 Am particles. It is seen that about 7% of particles deposit on the upper filters and about 20% deposit on the lower filters. These results also show that the total percentage of the deposited particles on the vessel wall and the outer surface of the shroud is about 60% due to the rotational motion and the importance of the centrifugal forces. It is also observed from Tables 1 and 2 that the percentages of deposited particles on the upper and

Table 1.

Percentage of the deposited 1 p m particles on different surfaces

1 Am particle (full shroud)	Percentage of deposited particles
Aborted Upper filter	0.6
Lower filters (perimeter)	8.1
Lower filter (central)	35.6
Vessel wall	4.6
Cone	25.9
	2.9
Inside of shroud	1.2
Outside of shroud	12.6
Central pipe	8.6
Top of casing	0

Table 2.

Percentage of the deposited 10 Am particles on different

1 Am particle (full shroud)	Percentage of deposited particles
Aborted Upper filter	0
Lower filters (perimeter)	6.9
Lower filter (central)	17.8
Vessel wall	3.5
Cone	48.3
	8.2
Inside of shroud	1.2
Outside of shroud	10.9
Central pipe	3.5
Top of casing	0.6

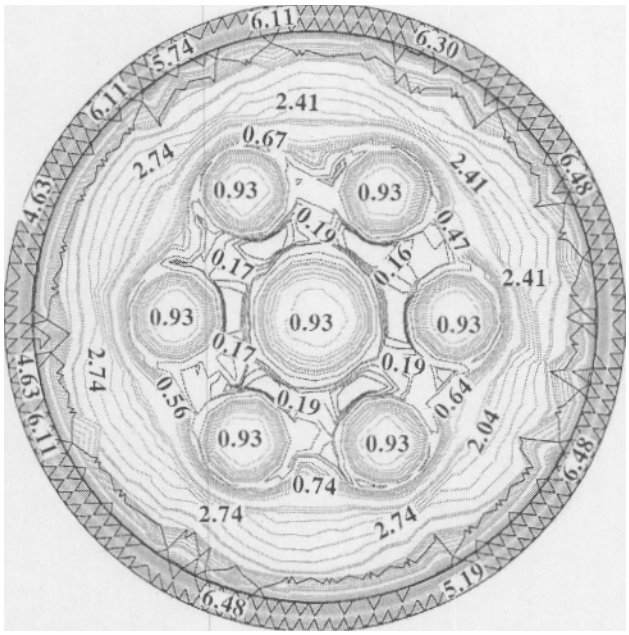

Figure 9. Mean velocity magnitude contours in a plane across the lower filters.

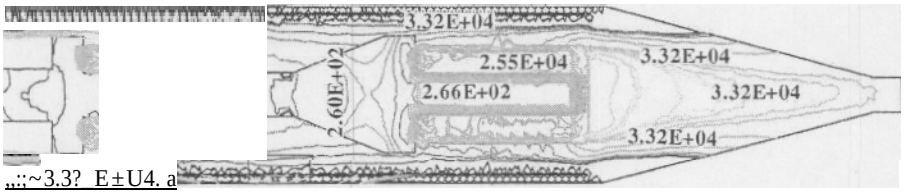

„:;~3.3? E±U4. a

Figure 10. Contour plot for variations of the static pressure at the; vessel mid-section.

Figure 11. Turbulence kinetic energy contours at the vessel mid-section.

lower filters decrease as the particle size increases. In addition, when particle size increases the deposition on the vessel wall increases, while deposition on the outer surface of shroud decreases.

6. CONCLUSION

In this work, particle transport and deposition in the hot-gas filter vessel at the PSDF at Wilsonville, Alabama is studied. The FLUENT code is used to simulate the mean turbulent flow field and the corresponding particle trajectories. On the basis on the presented results, the following conclusions are drawn:

. The gas velocity magnitude inside the shroud is generally high, while it is relatively low inside the vessel.

. The main pressure drop occurs across the filter wall.

. The turbulent kinetic energy is generally quite low in the vessel, except for certain regions inside the connecting tube.

. Particles are transported by the highly swirling flows from the inlet moving both in upward and downward directions through the shroud, and then enter the main body of the vessel.

. The rotational motion and centrifugal forces are quite important for particle deposition rates in the filter vessel.

. The total number of particles that deposit on the filters and on the central post including the tube sheet decreases as particle diameter increases.

For the startup condition (clean filters with a constant permeability), the particle deposition rate on the lower tier filters is larger than that on the upper tier filters.

. Since the central post and the tube sheet surfaces have no cleaning mechanism, there is a potential for ash buildup and initiation of ash bridging due to particle deposition in these regions.

. The simulation shows that a small fraction of particles could penetrate the filter cluster and deposit on the central post during the steady state filtration process.

Acknowledgements

The authors would like to thank John Foote and Xiaofeng Guan of Southern Company Services, Zal Sanjana, Theodore McMahon and Richard Dennis for many helpful discussions. The work of G. Ahmadi was supported by DOE grant DEFC26-98T4047. Thanks are also given to FLUENT Corporation for making the code available.

REFERENCES

1. J. M. Rockey *et al.*, High temperature high pressure filtration and sorbent program, *METC/Shell CooperativeAgreement, CRADA 93-011, Vols I* and II, Morgantown Energy Technology Center, Morgantown, WV (1995).
2. D. H. Smith, V. Powell, G. Ahmadi and H. Ibrahim, Analysis of operational filtration data - Part I: Ideal candle filter behavior, *Powder Technol.* 94, 5-2.1 (1997).
3. D. H. Smith, G. J. Haddad and U. Grimm, Composition and chemistry of particulates from a PFBC demonstration plant, *Fuel* 76, 727-732 (1997).
4. D. H. Smith, V Powell and G. Ahmadi, Analysis of operational filtration data - Part 11: Incomplete filter cleanine. *Powder Technol.* 97. 139-145 (1998).
5. D. H. Smith, V. Powell, G. Ahmadi and M. Ferer, Analysis of operational filtration data-Part III: Re-entrainment and incomplete cleaning of dust cake, *Aerosol Sci. Technol.* 29, 224-235 (1998).
6. M. J. Mudd and J. D. Hoffman, Initial operation of the Tidd PFBC hot-gas clean up filter, in: *Proc. Coal-Fired Power Systems '93 - Advances in .IGCC and PFBC Review Meeting,* D. L. Bonk (Ed.), pp. 483-495, DOE/METC-93 /6131. US Department of Energy, Morgantown Energy Technology Center, Morgantown, WV (1993).
7. M. J. Mudd and J. D. Hoffman, Tidd PFBC hot-gas filter operation experience: July 1993-April 1994, in: *Proc. Coal-Fired Power Systems '94 -Advances in IGCC and PFBC Review Meeting,* H. M. McDaniel, R. K. Staubly and V. K. Venkataraman (Eds), DOE/METC-94/1008. US Department of Energy, Morgantown Energy Technology Center, Morgantown, W V (1994).
8. T. E. Lippert, G. J. Bruck, E. E. Smeltzer, R. A. Newby and D. M. Bachovchin, Westinghouse filter update, in: *Proc. Coal-Fired Power Systems '93 - Advances in IGCC and PFBC Review Meeting,* D. L. Bonk (Ed.), pp. 497-512, DOE/METC-93/6131. US Department of Energy, Morgantown Energy Technology Center, Morgantown, WV (1993).
9. T. E. Lippert, G. J. Bruck, Z. N. Sanjana and R. A. Newby, Westinghouse advanced particle filter system, in: *Proc. Coal-Fired Power Systems '94 - Advances in IGCC and PFBC Review Meeting,* H. M. McDaniel. R. K. Staubly and V. K. Venkataraman (Eds), pp. 152-165, Vol. I, DOE/METC-94/1008. US Department of Energy, Morgantown Energy Technology Center, Morgantown, WV (1994).
10. T. E. Lippert, W. F. Domeracki and V. L. Debski, The status of Westinghouse hot gas particle filters and testing results, in: *Power-Gen Americas '95,* Anaheim, California (1995).
11. Southern Research Institute, Assessment of ash characteristics from gas stream cleanup facilities, *Topical Report,* Contract DEAC21-89MC26239 (1993).
12. D. H. Pontius, Hot-gas filtration technical issues, in: *Proc. Coal-Fired Power Systems '95 Review Meeting,* H. M. McDaniel, D. Mollot and V. K. Venkataraman (Eds), pp. 531-546, DOE/METC-95/1018. US Department of Energy, Morgantown Energy Technology Center, Morgantown, WV (1995).
13. J. P. Hurley, T. M. Strobel and B. A. Docter, Hot-gas filter ash characterization, in: *Proc. CoalFired Power Systems '95 Review Meeting,* H. M. McDaniel, D. Mollot and V. K. Venkataraman (Eds), pp. 449-463, DOE/METC-95/1018. US Department of Energy, Morgantown Energy Technology Center, Morgantown, WV (1995).
14. M. Davidson, X. Guan, H. Hendrix and P. Scarborough, Power system development facility: High temperature, high pressure filter system operation in conabustion gas, in: *High Temperature Gas Cleaning,* A. Dittler, G. Hemmer and G. Kasper (Eds), Vol. 11, pp. 315-334. Braun, Karlsruhe (1999).
15. K. V. Thambimuthu, Gas cleaning for advanced coal-based power generation, *EACR/53,* IEA Coal Research, London (1993).
16. R. Clift and J. P. K. Seville, *Gas Cleaning at High Temperatures.* Blackie, New York (1993).

17. E. Schmidt, P. Gang, T. Pilz and A. Dittler, High Temperature Gas Cleaning. Institute fur Mechanische Verfahrenstechnikund Mechanik, Karlsruhe (1996).
18. A. Dittler, G. Hemmer and G. Kasper (Eds), High Temperature Gas Cleaning, Vol II. Braun, Karlsruhe (1999).
19. Smith and Ahmadi (1995).
20. S. K. Friedlander and H. H. Johnstone, Deposition of suspended particles from turbulent gas streams, Ind. Engng. Chem. 49, 1151-1156 (1957).
21. Cleaver and Yates (1975).
22. N. B. Wood, A simple method for the calculation of turbulent deposition to smooth and rough surfaces, J. Aerosol Sci. 12, 275-290 (1981).
23. N. B. Wood, The mass transfer of particles and acid vapor to cooled surfaces, J. the Institute of Energy 76, 76-93 (1981).
24. W. C. Hinds, Aerosol Technology. John Wiley & Sons, New York
(1982). 25. G. M. Hidy, Aerosol. Academic Press, New York (1984).
26. P. G. Papavergos and A. B. Hadley, Particle deposition behavior from turbulent flows, Chemical EngineerRes. Des. 62, 275-295 (1984).
27. F.-G. Fan and G. Ahmadi, A sublayer model for turbulent deposition of particles in vertical ducts with smooth and rough surfaces, J. Aerosol Sci. 24, 45-64 (1993).
28. Li and Ahmadi (1993).
29. A. Li, G. Ahmadi, R. G. Bayer and M. A. Gaynes, Aerosol particle deposition in an obstructed turbulent duct flow, J. Aerosol Sci. 25, 91-112 (1994).
30. A. Li, G. Ahmadi, M. A. Gaynes, and R. G. Bayer, Aerosol particle deposition in a recirculating region, J. Adhesion 51, 87-103 ('1995).
31. C. He and G. Ahmadi, Particle deposition in a nearly developed turbulent duct flow with electrophoresis, J. Aerosol Sci. 30, 739-758 (1999).
32. G. Ahmadi and D. H. Smith, Particle transport and deposition in a hot-gas cleanup pilot plant, Aerosol Sci. Technol. 29, 183-205 (1998).
33. G. Ahmadi and D. H. Smith, Gas flow and particle deposition in the hot-gas filter vessel at the Tidd 70 MWE PFBC demonstration power plant, Aerosol Sci. Technol. 29, 206-223 (1998).
34. H. Zhang and G. Ahmadi, Particle transport and deposition in the hot-gas filter vessel at Wilsonville, Powder Technol. 116, 53-68 (2001).
35. 1. K. Gamwo, G. Ahmadi and J. S. Halow, Non-isothermal simulation of gas flows in the hot-gas filter vessel at Wilsonville, Part. Sci. Technol. (2002) (in press).
36. G. Ahmadi and D. H. Smith, Computational modeling of particle transport and deposition in hot-gas cleanup filter vessels, in: Proc. 2nd Int. Symp. on Scale Modeling (ISSM-II), Lexington, KY, pp. 337-350 (1997).